

# Applications of Profile Filtering in the Dimensional Metrology of Fuel Cell Plates

Bala Muralikrishnan, Wei Ren, Eric Stanfield, Dennis Everett, Alan Zheng, and Ted Doiron  
Semiconductor and Dimensional Metrology Division  
National Institute of Standards and Technology, Gaithersburg MD 20899

## Abstract

We describe the application of several surface profile filters as an enabling tool in the dimensional measurements of an engineering artifact, namely, a fuel cell plate. We recently reported work on the development of a non-contact system for dimensional metrology of bipolar fuel cell plates. That system is comprised of two laser spot triangulation probes that acquire profile data across a plate. While the non-contact system provides rapid measurements (measurement speed of 100 mm/s to 500 mm/s), the data are noisy and cannot be used directly to obtain features of interest such as channel depth and width. In this paper, we show how different surface profile filters such as the spline, morphological, and robust filters, can be employed to identify and suppress outliers and to produce a mean line that serves as a substitute geometry from which we can determine features of interest. Further, we compare the non-contact probe data against contact probe measurements made using a coordinate measuring machine (CMM). Surface profile filters are again useful in correcting the reference data for tip size and also in removing any free form deformation in both data sets prior to parameter evaluation and comparison.

## 1. Introduction

Surface finish and key dimensions of engineering components are indicators of the stability of a manufacturing process [1] and are therefore constantly monitored during their manufacture. While such measurements are sometimes performed off-line in an inspection facility, increasingly manufacturers are attempting to employ in-process inspection to not only save time and cost, but to also ensure that 100 % of the components are inspected.

In this context, we recently reported work [2] on the development of a non-contact measurement system for dimensional metrology of bipolar fuel cell plates. While contact probe systems are accurate, complete dimensional measurement of a single plate using a coordinate measuring machine (CMM) could take several minutes or even hours. To address the measurement time issue, we developed a unique dual probe laser triangulation-based system and demonstrated measurements that can be performed with high accuracy and at extremely high speeds; a plate measurement can be completed in less than a minute. While the system offers considerable speed, the data are noisy and cannot be used directly to obtain features of interest such as channel depth and width. In this paper, we show how different surface profile filters can be employed to identify and suppress outliers and to produce a mean line that serves as a substitute geometry from which we can determine features of interest.

In general, profile filters are used in surface texture analysis for the separation of different wavelength regimes such as roughness, waviness and form. Parameters are computed in each regime and then used for correlation with part functionality or to provide information on

manufacturing process stability [1]. In this paper, we describe the application of profile filters as an enabling tool in the dimensional measurements of fuel cell plates. We show how several surface profile filters such as the spline, the morphological, and the robust Gaussian regression [3-8], can all be employed to identify and suppress outliers, to create substitute geometry, and even to correct the reference data for probe tip convolution effect. We also show how these filters can be used to remove form, which in this case refers to the free form geometry of the plate. We describe the application and reference data in the next section, the non-contact probe data in section 3, a comparison in section 4, and finally present conclusions in section 5.

## 2. The fuel cell plate and reference data analysis

### 2.1 The plate

A photo of the fuel cell plate similar to the one considered in this study is shown in Fig. 1. It is about 70 mm x 50 mm in size and is fairly thin and flexible. The channels are approximately 2 mm wide at the top, 0.6 mm deep. The plate is made of 0.3 mm thick aluminum. The channels have a free form profile, see Fig. 2(a); such profiles can be obtained from a number of processes such as stamping, chemical etching, etc. Analysis techniques described in this paper are applicable to all such plates.

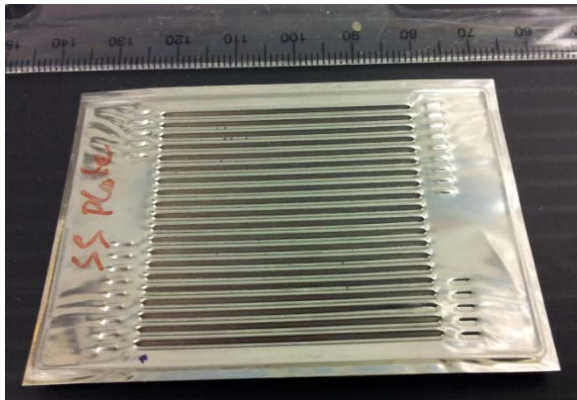


Fig. 1 Photo of fuel cell plate

### 2.2 Raw profile and spline mean line

The reference data for this study are acquired using a Mitutoyo<sup>1</sup> UMAP fiber probe based CMM. The probe stem is 20  $\mu\text{m}$  in diameter and 2 mm long, and has a 30  $\mu\text{m}$  diameter ball at the end. The raw profile data, acquired with a spacing of 5  $\mu\text{m}$ , is shown in Fig. 2(a). Its Fourier spectrum is shown in Fig. 2(b). The plots show a dominant 2 mm wavelength component, which corresponds to the channel pitch. The long wavelength components (or form), larger than 8 mm in wavelength, correspond to the free form of the flexible channel. At the high frequency (short

---

<sup>1</sup> Commercial equipment and materials may be identified in order to adequately specify certain procedures. In no case does such identification imply recommendation or endorsement by the National Institute of Standards and Technology, nor does it imply that the materials or equipment identified are necessarily the best available for the purpose.

wavelength) end of the spectrum, there are small peaks (amplitude smaller than 0.05 mm) between 0.2 mm and 1 mm in wavelength.

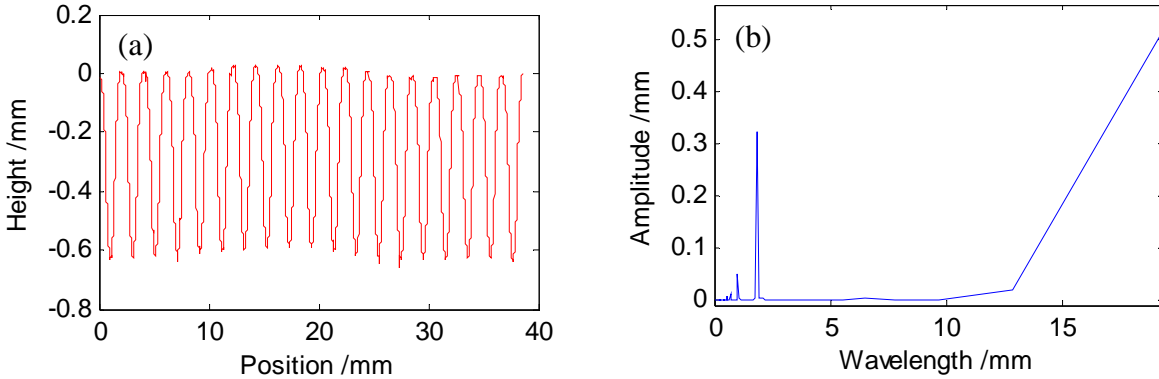


Fig. 2 (a) Raw profile obtained by the CMM (b) Fourier spectrum of the profile

The Fourier spectrum is useful in selecting appropriate cutoffs for the different filters employed in processing the data. For example, as a first step in the analysis of the reference data, we create a spline mean line to smooth out the noise in the high frequency end of the spectrum. For this purpose, we select a filter with a cutoff of 0.08 mm. This value is chosen so that it is smaller than the first significant peak in the Fourier spectrum which occurs at a wavelength of 0.17 mm. Further, it belongs to the preferred set of values for cutoffs as stated in the ASME B46.1 [9], which are 0.08 mm, 0.25 mm, 0.8 mm, 2.5 mm, and 8 mm. The spline mean line is shown in Fig. 3 along with the raw data. The spline mean line is used in subsequent processing of the data, i.e., in correcting for probe tip effects and in removing the free form geometry of the plate.

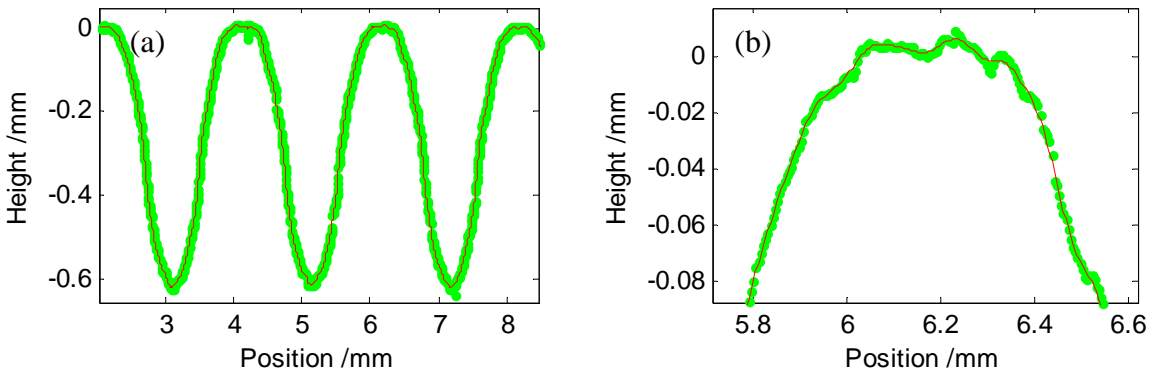


Fig. 3 (a) Contact probe CMM data and spline mean line across the first few channels of the plate (b) close up view near the peak of one channel

### 2.3 Probe tip correction

The coordinates recorded by a CMM probing system upon contact with the surface generally represent the center of the probe ball. The surface coordinate is then determined by a procedure known as probe radius compensation, which involves advancing the coordinate by an amount equal to the probe radius along the probing direction. This procedure is only valid if the actual contact point on the probe happens to be collinear with the probing direction vector. That is, the local surface normal is along the probing direction. When the form changes rapidly but the

probing direction remains the same, the point of contact on the probe ball is no longer where expected, and the radius compensation procedure yields a surface coordinate that could be very different from the true surface coordinate. This is illustrated in Fig. 4 where the probe makes contact with the surface at point A. Because the probing direction is along the negative Z axis, the apparent measured surface point (after probe radius compensation) is point C, which is different from the true surface point, point B.

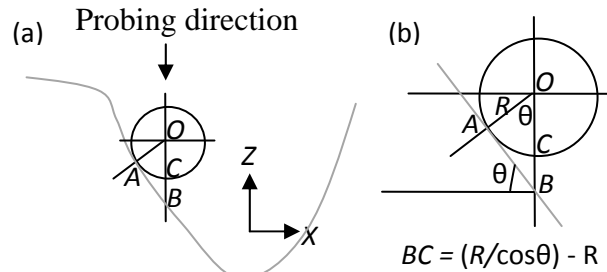


Fig. 4 (a) Error in contact probe measurements due to finite probe size (b) Estimation of error for a straight edge

The magnitude of the error along Z shown by the distance BC in Fig. 4 can be estimated from the surface slope and the size of the probe ball. The side wall slope of the channels is  $45^\circ$  and the radius of the probe ball is  $15 \mu\text{m}$ . Assuming the surface is a straight edge, the error in the determination of the surface coordinate BC is about  $6 \mu\text{m}$ , which is a fairly large error. We therefore correct the measured data using morphological erosion operation to determine more accurate surface coordinates, instead of simply doing a probe radius compensation along the probing direction.

The resulting profile is substantially different at the side walls as seen in Fig. 5. The measured center of the probe ball is shown in Fig. 5 as the red line with dots. The CMM software compensates for the probe radius along the probing direction to produce the surface shown by the light gray line. This is an incorrect location for the surface. A morphological erosion operation on the measured centers of the probe ball produces the solid blue line shown in the figure. The two parameters for the erosion filter are the probe ball radius and spacing. The probe ball radius is nominally  $15 \mu\text{m}$  (the true value is to within about  $0.1 \mu\text{m}$  of the nominal) and the spacing between points is  $5 \mu\text{m}$ . Notice how the morphological erosion line is displaced from the profile produced by compensating along the probing direction, thus reducing the error in the location of the surface profile.

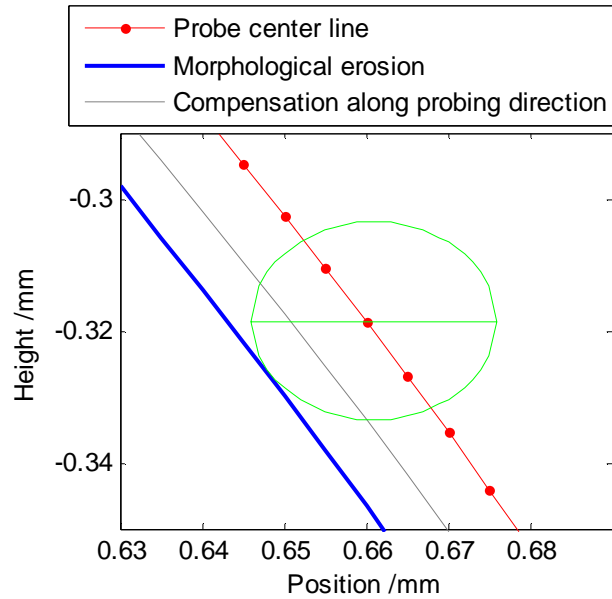


Fig. 5 Probe center line, profile generated by performing a compensation along the probing direction by an amount equal to one radius, profile generated by morphological erosion.

## 2.4 Free form deformation removal

The plate, as mentioned earlier, is flexible and appears to have some form. In order to compare the profiles obtained from the non-contact and the contact probe measurements, we remove this free form geometry using a long wavelength filter. It is known that the Gaussian and the spline filters suffer from edge distortion. Generally, a length equal to half the cutoff has to be discarded from both ends. Given that the filter to be used here will have a large cutoff (a value of 8 mm is chosen from the preferred set mentioned earlier), the use of spline and Gaussian filters will require 4 mm of data from each end to be discarded; this is a substantial portion of the total measured length. Robust filters, on the other hand, do not suffer from edge distortion, and the entire profile length may be used for further analysis. We therefore employ a robust Gaussian regression filter [10], with a cutoff of 8 mm, to generate the form profile (see Fig. 6(a)). We then subtract this form profile to obtain a profile which we use as the reference profile (Fig. 6(b)). The choice of cutoff is application dependent; it is not possible to make a general suggestion that will fit all applications. Seewig [9] recommends a cutoff of three times the feature width for the successful application of the Gaussian regression filter. As discussed earlier in section 2.2, we choose 8 mm as the form cutoff for the robust filter because the Fourier spectrum suggests that the wavelengths corresponding to the free-form plate deflections are greater than this value, and 8 mm happens to be a part of the preferred series of cutoff values in the ASME B46.1 Standard.

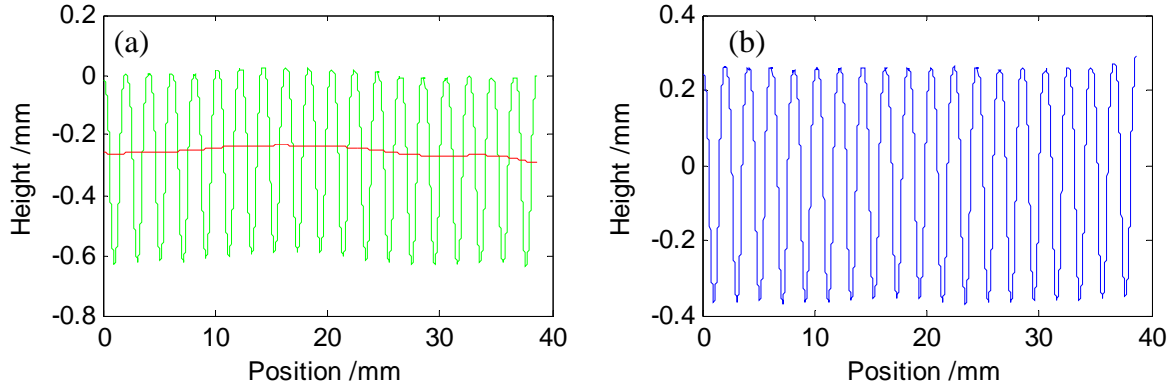


Fig. 6 (a) Probe radius corrected profile and robust Gaussian regression mean line generated with 8 mm cutoff (b) Mean line removed profile for comparison with non-contact measurement

### 3. Non-contact probe data analysis

#### 3.1 Outlier identification and creation of substitute geometry

The non-contact data are acquired at the same sampling interval of 5  $\mu\text{m}$  as the CMM data. The nominal spot size of the probe at the center of its range is 30  $\mu\text{m}$ . The spot size is not a constant but increases farther with increasing range. Prior to performing the plate measurements, the plate was aligned so that the probe was at or near the center of its range throughout the length of the plate.

Before we proceed, we note that it is rather challenging to identify the precise location on the plate where the contact probe measurements were made, so that we can then measure at that location using our non-contact system. Using some fiducials, we can locate the position of the contact probe measurements to within  $\pm 0.5$  mm. What we therefore do is to measure several parallel traces in that region and study the variability in the profiles. What we have noticed is that the repeatability in those profiles is much smaller than the observed differences between the non-contact and contact probe systems. Therefore, we know that form of the plate is consistent in the region of about  $\pm 0.5$  mm, and we can therefore use any of those profiles, or better yet, the average of three profiles, as the result of the non-contact measurement.

The non-contact probe data are noisy, see Fig. 7. In addition, the data at the bottom of the channels show several streaks due to secondary reflections. The first task in the analysis of these data is to identify and remove outliers, and to create a substitute geometry. For this purpose, we first generate a mean line using the robust Gaussian regression filter with 0.08 mm cutoff. The robust filter is not influenced by small outliers and produces a mean line that reasonably hugs the texture. It may still be influenced somewhat by the large streaks of data at the bottom of the channels. In order to identify the data that comprise these large streaks and outliers, we then create two profiles that are displaced by a certain threshold (chosen by trial and error as 30  $\mu\text{m}$ ; this value is chosen to allow small surface features to remain while omitting large outliers) from the Gaussian regression mean line. Simply translating the Gaussian regression mean lines above and below will produce an unequal spacing at the sidewalls and the top/bottom because of the different surface slopes. We therefore create morphological dilation and erosion profiles from the Gaussian regression profile; these serve as the upper and lower limits for the data points that

represent the actual surface. Any points lying outside these limits are considered as outliers and are discarded. We then filter the resulting data set using a spline filter with 0.08 mm cutoff to obtain the substitute geometry.

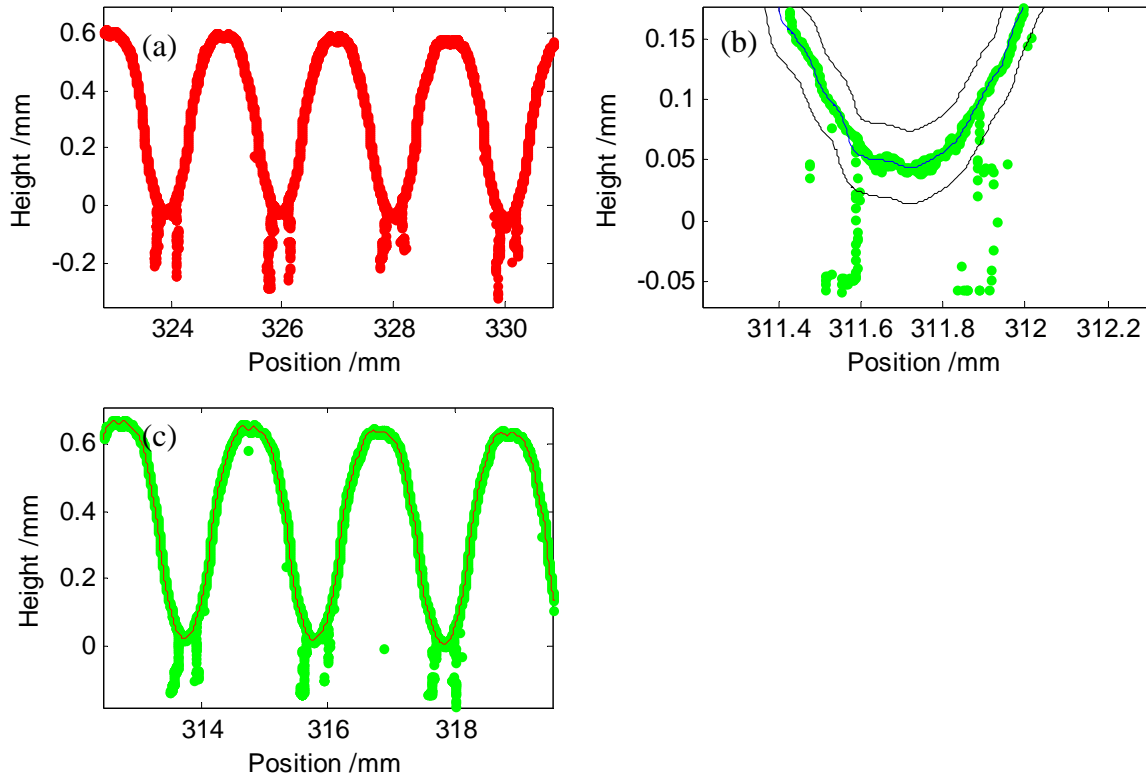


Fig. 7 (a) Raw profile from non-contact system (b) robust Gaussian regression mean line along with an upper and lower boundary profiles for outlier identification (c) Spline mean line (the red line) after outlier identification and removal.

### 3.2 Free form deformation removal

As discussed in section 2.4, we remove the free form geometry of the plate using a robust Gaussian regression filter of 8 mm cutoff. The robust filter is not sensitive to edge effects and therefore, we do not have to discard the first and last half cutoffs. The profile and the robust Gaussian regression mean line are shown in Fig. 8(a), and the form removed profile is shown in Fig. 8(b).

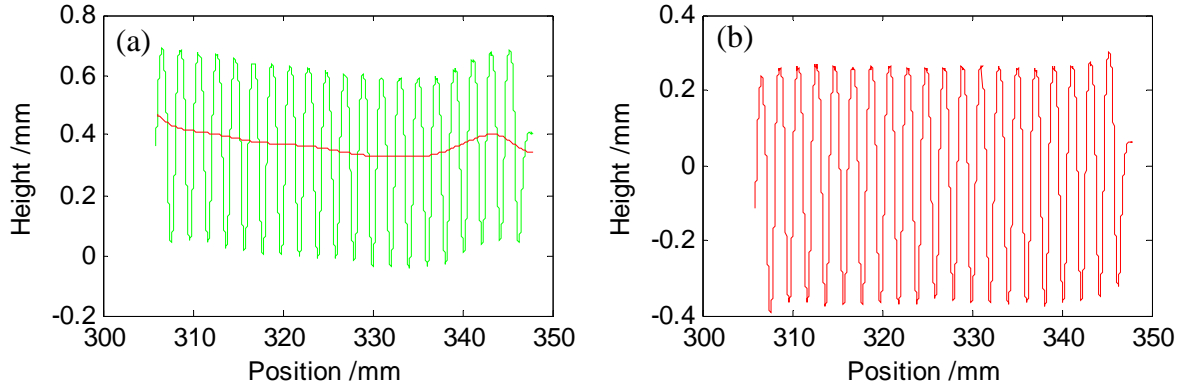


Fig. 8 (a) Profile and the robust Gaussian regression mean line with 8 mm cutoff (b) Form removed profile

#### 4. Comparison and parameter evaluation

The form removed profiles obtained from both the CMM and the non-contact probe are shown in Fig. 9. Because the two profiles are obtained from different instruments and therefore different coordinate systems, we determine the best overlap position using cross correlation. We then determine the vertical point-to-point differences between the profiles. The mean and standard deviation of these point-to-point differences are  $1.5 \mu\text{m}$  and  $10 \mu\text{m}$ , respectively. Most of the large differences happen at the side walls where the non-contact probe measures the surface at a grazing angle and therefore produces larger measurement errors [11]. The small value for the mean difference suggests that there is no bias (or vertical shift) between the two profiles.

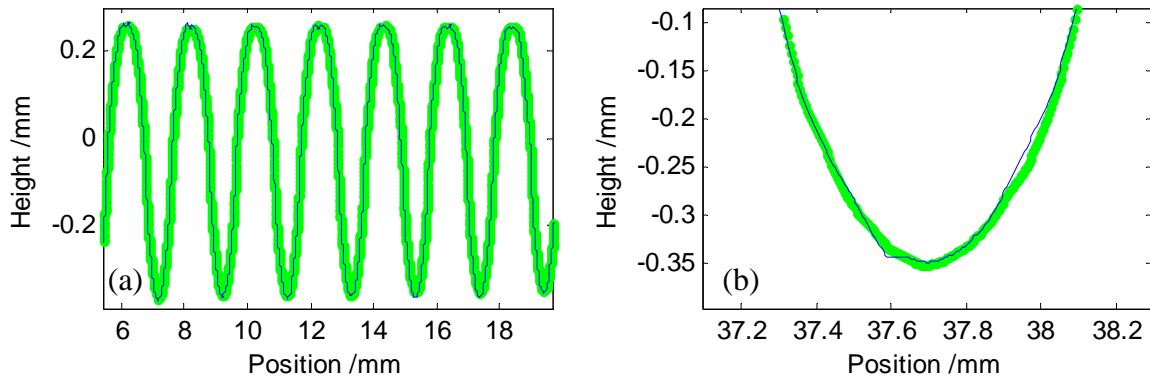


Fig. 9 Form removed profiles from both the CMM (shown as a series of green dots) and the non-contact probe (shown as a solid blue line) (a) over a 14 mm portion of the profile (b) over just a 0.8 mm portion of the profile

We define channel height as the distance between the average  $Z$  position of the two consecutive peaks to the valley between them. Because the channels have no land area, we consider the average over a  $0.1 \text{ mm}$  region, centrally located at the peak or valley, as the measure of the  $Z$  position. We calculate the channel heights for each of the seventeen channels, for both the CMM and the non-contact probe data, and then compute the differences. These differences range from  $-8 \mu\text{m}$  to  $15 \mu\text{m}$ , with a mean difference of  $5 \mu\text{m}$  and a standard deviation of  $6 \mu\text{m}$ . The positive mean difference of  $5 \mu\text{m}$  suggests that the non-contact probe may be estimating channel heights



slightly larger than the contact probe CMM measurements, but nevertheless, this value is small in comparison to the linearity of the probes themselves, which is specified at  $\pm 5 \mu\text{m}$ .

We also calculate the channel widths at different heights for the two profiles. At the  $Z = 0$  height, the differences in the widths of the seventeen channels has a mean of  $4 \mu\text{m}$  and a standard deviation of  $19 \mu\text{m}$ . The spread in values is rather large, but it should be noted that small changes in local slopes will affect the width in that vicinity. As mentioned earlier, side wall measurement is a challenge because the laser is incident at a grazing angle and therefore more prone to measurement errors. This is a limitation of the measurement technology.

We have not determined a detailed uncertainty budget for height and width at this time. The primary objective of this paper is on the analytical techniques used to process high density non-contact data that has outliers. The primary sources of uncertainty in our measurement are associated with the probe; the analytical techniques used do propagate that uncertainty into the measurands (height and width). The general tolerances on the dimensions of these plates range anywhere from  $50 \mu\text{m}$  to as low as  $12 \mu\text{m}$  [12]. If the tolerances are as high  $50 \mu\text{m}$ , we believe non-contact systems will be adequate for shop floor use. On the other hand, as tolerances reduce to the  $10 \mu\text{m}$  level, non-contact systems have to be more carefully studied to identify error sources so that their accuracies are further improved.

## 5. Conclusions

Profile filtering is generally used in surface texture analysis to partition a profile into different wavelength regimes such as roughness, waviness, and form. In dimensional analysis of high density data, filtering techniques can be applied to not only suppress measurement noise, but also used in outlier identification and removal and in the creation of a substitute geometry. In this paper, we show how several surface profile filters [13-16] can be employed as enabling tools in the dimensional measurement of a fuel cell plate, where high density data are acquired using non-contact probes. We demonstrate how robust Gaussian regression and spline filters may be used to identify and suppress outliers and create a substitute geometry from which parameters of interest such as channel depth and width may be evaluated. In addition, we acquire high density data from a contact probe to establish the validity of the non-contact probe measurements. We show how morphological filters are useful in correcting probe tip effects, and also show how the free form geometry of these flexible plates can be corrected using Gaussian regression filters without loss of edge data.

With the increasing trend towards 100 % part inspection, manufacturers will rely on non-contact measurement for its speed and high data density. With such high density dimensional data, the distinction between dimensional and surface texture analysis will become less marked, and filtering techniques will be more commonly applied in the dimensional measurement and analysis of engineering artifacts.

## Acknowledgements

We thank Chris Blackburn and George Orji at NIST and Jay Raja at UNCC for reviewing the manuscript.

## References

1. Whitehouse D.J., Surface Metrology, Meas. Sci. Technol, 1997, **8** 955-972
2. B. Muralikrishnan, W. Ren, D. Everett, E. Stanfield, T. Doiron, Dimensional Metrology of Bipolar Fuel Cell Plates Using Laser Spot Triangulation Probes, Measurement Science and Technology, 22(7), July 2011
3. Krystek M. Discrete linear profile filters. Proceedings of the X. International Colloquium on Surfaces, Chemnitz University of Technology, Chemnitz, 2000, 145-152.
4. Krystek M. Form filtering by splines. Measurement 1996;18;9-15.
5. Brinkmann S, Bodschwinn H, Lemke HW. Development of a robust Gaussian regression filter for three-dimensional surface analysis. Proceedings of the X. International Colloquium on Surfaces, Chemnitz University of Technology, Chemnitz 2000, 122-132.
6. Srinivasan V. Discrete Morphological filters for Metrology. Proceedings of the 6<sup>th</sup> IMEKO ISMQC Symposium on Metrology for Quality Control in Production, TU Wien, Austria, 1988.
7. J.Raja, B.Muralikrishnan and Shengyu Fu , Recent advances in separation of roughness, waviness and form, Precision Engineering – Journal of the International Societies for Precision Engineering and Nanotechnology, 26 (2), 2002, 222-235
8. B. Muralikrishnan and J. Raja, Computational Surface and Roundness Metrology, Springer-Verlag, London, UK, ISBN 978-1-84800-296-8, 2008
9. ASME B46.1-2002, Surface Texture (Surface roughness, waviness, and lay)
10. J. Seewig, Linear and robust Gaussian regression filters, 2005 J. Phys.: Conf. Ser. 13 254
11. B. Muralikrishnan, W. Ren, D. Everett, E. Stanfield, T. Doiron, Performance evaluation experiments on a laser spot triangulation probe, Measurement: Journal of the IMEKO, 45(3) 2012, 333-343
12. Eric Stanfield and Mike Stocker, Metrology for fuel cell manufacturing, 2012 DOE hydrogen and fuel cells program review, May 16<sup>th</sup> 2012, presentation available at [http://www.hydrogen.energy.gov/pdfs/review12/mn006\\_stanfield\\_2012\\_o.pdf](http://www.hydrogen.energy.gov/pdfs/review12/mn006_stanfield_2012_o.pdf), accessed 4/16/2013
13. ISO/TS 16610-22:2006, Geometrical product specifications (GPS) -- Filtration -- Part 22: Linear profile filters: Spline filters
14. ISO/TS 16610-31:2010, Geometrical product specifications (GPS) -- Filtration -- Part 31: Robust profile filters: Gaussian regression filters
15. ISO/TS 16610-40:2006, Geometrical product specifications (GPS) -- Filtration -- Part 40: Morphological profile filters: Basic concepts
16. ISO/TS 16610-41:2006, Geometrical product specifications (GPS) -- Filtration -- Part 41: Morphological profile filters: Disk and horizontal line-segment filters

